Am J Cancer Res 2025;15(12):5245-5255
www.ajcr.us /ISSN:2156-6976/ajcr0169517

Original Article

Comparison of intravenous contrast-enhanced ultrasound and magnetic resonance imaging in preoperative staging of endometrial carcinoma

Shuang Guo[1,2], Huidong Li[2], Hong Yu[3], Jingwen Si[4], Tong Wang[2], Zhaoxiang Ye[1]

[1]Department of Radiology, Tianjin Medical University Cancer Institute and Hospital, National Clinical Research Center for Cancer; Tianjin's Clinical Research Center for Cancer; State Key Laboratory of Druggability Evaluation and Systematic Translational Medicine; Key Laboratory of Cancer Prevention and Therapy, Tianjin 300060, China; [2]Department of Ultrasound, Tianjin Central Hospital of Gynecology Obstetrics, Tianjin 300100, China; [3]Department of Radiology, Tianjin Central Hospital of Gynecology Obstetrics, Tianjin 300100, China; [4]Department of Pathology, Tianjin Central Hospital of Gynecology Obstetrics, Tianjin 300100, China

Received October 24, 2025; Accepted December 2, 2025; Epub December 15, 2025; Published December 30, 2025

Abstract: Background: Accurate preoperative staging of endometrioma (EC) is essential for optimal treatment planning. This study aims to evaluate the diagnostic performance of intravenous contrast-enhanced ultrasound (IV-CEUS) as a potential modality for EC staging. Methods: This retrospective study involved 71 patients with histologically confirmed EC who were admitted to Tianjin Central Hospital of Gynecology Obstetrics between January 2021 and August 2024. All patients had undergone both IV-CEUS and magnetic resonance imaging (MRI) within 14 days before surgery. IV-CEUS was performed using high-end Doppler ultrasound systems with SonoVue® contrast, while MRI was conducted on a 1.5 T scanner employing T2 weighted, diffusion-weighted, and dynamic contrast-enhanced sequences. Deep myometrial invasion (DMI; ≥ 50%) and cervical stromal invasion (CSI) were assessed, with final histopathological findings serving as the reference standard. Diagnostic performance was evaluated using sensitivity, specificity, predictive values, accuracy, Kappa coefficients, and receiver operating characteristic (ROC) curves. Results: For DMI diagnosis, IV-CEUS demonstrated a sensitivity of 74.2%, specificity of 92.5%, PPV of 88.5%, NPV of 82.2%, and accuracy of 84.5% (κ = 0.68). MRI showed a sensitivity of 90.3%, specificity of 85.0%, and accuracy of 87.3% (κ = 0.75). For CSI diagnosis, IV-CEUS had a sensitivity of 69.2%, specificity of 93.1%, an accuracy of 88.7% (κ = 0.62), while MRI had a sensitivity of 76.9%, specificity of 87.9%, and accuracy of 85.9% (κ = 0.60). The areas under the curves (AUCs) were 0.704 (95% CI: 0.584-0.824) for IV-CEUS and 0.718 (95% CI: 0.602-0.834) for MRI in diagnosing DMI; and those were 0.852 (95% CI: 0.743-0.961) for IV-CEUS and 0.838 (95% CI: 0.721-0.955) for MRI in diagnosing CSI. Conclusion: IV-CEUS demonstrates comparable diagnostic performance to MRI in assessing DMI and CSI in EC patients. It may serve as a viable alternative when MRI is contraindicated or unavailable.

Keywords: Endometrial cancer, intravenous contrast enhanced ultrasound, magnetic resonance imaging, deep myometrial invasion, cervical stromal invasion

Introduction

Endometrial cancer (EC) is one of most prevalent gynaecological malignancies worldwide, ranking fourth among glandular tumors [1]. Its incidence is rising due to aging populations, increasing obesity, metabolic disorders, and declining fertility rates, making timely and accurate diagnosis imperative [2, 3]. Early detection and precise preoperative staging are crucial for optimizing treatment planning and improving outcomes [4]. The 5-year survival rate exceeds 85% for stage I disease but drops to 22%-51% for stage III and above [5]. Key staging parameters, including the depth of myometrial invasion and cervical stromal involvement (CSI), play a central role in guiding surgical management and predicting prognosis.

Histopathological diagnosis via curettage or surgery excision remains the gold standard for EC confirmation [6]. However, curettage is invasive and blind, potentially overlooking small or focal lesions, and carrying risks of bleeding,

https://doi.org/10.62347/LBAI6307

tumor dissemination, and infection, which may limit its utility in some cases [7]. Currently, pelvic magnetic resonance imaging (MRI) is the most widely used imaging modality for preoperative staging of EC [8]. MRI offers high spatial resolution and excellent soft-tissue contrast, facilitating the assessment of deep myometrial invasion (DMI), CSI, and suspected lymph node metastases [8, 9]. Nevertheless, MRI has several limitations, including high cost, long acquisition times, limited accessibility in resource-constrained settings, and contraindications such as severe claustrophobia or metallic implants (e.g., pacemakers). In patients with renal impairment, the use of gadolinium-based contrast agents is also restricted [10]. Additionally, the accuracy of MRI may be compromised by coexisting uterine conditions such as adenomyosis or leiomyomas, which can obscure the tumor-myometrium interface [11].

In this context, contrast-enhanced ultrasound (CEUS) has emerged as promising non-invasive modality for real-time dynamic assessment of microvascular tumor perfusion [12]. According to the European Federation of Societies for Ultrasound in Medicine and Biology (EFSUMB) guidelines, the intravenous CEUS (IV-CEUS) criteria for DMI include disruption of the subendometrial enhancement ring and tumor extension of ≥ 50% into the myometrium [13]. For CSI, the loss of normal cervical stromal enhancement and direct tumor extension into the stroma are key indicators [14]. Perfusion characteristics such as early heterogeneous enhancement, high peak intensity, and early wash-out have been associated with aggressive tumor behavior [12]. IV-CEUS, which involves peripheral injection of microbubble agents (e.g., SonoVue®), enables continuous, non-invasive visualization of tumor perfusion within the uterine cavity [15]. IV-CEUS combines the advantages of transabdominal/transvaginal ultrasound with real-time microcirculation assessment, while avoiding ionizing radiation and offering shorter examination times and lower costs [16]. It is particularly attractive for repeated evaluations and in settings where MRI is unavailable or contraindicated (e.g., patients with metallic implants, renal insufficiency, or claustrophobia) [17]. CEUS is routinely used in liver imaging to differentiate benign from malignant lesions based on arterial enhancement and wash-out patterns [18]. In breast imaging, it has shown potential in distinguishing malignant from benign masses through contrast kinetics and vascular architecture evaluation [19].

Despite these advantages, the use of IV-CEUS in gynecologic oncology, especially for preoperative EC staging, remains underdeveloped and is not yet standard clinical practice [14]. Limited studies have specifically investigated its efficacy in evaluating DMI and CSI in EC, and comparative studies directly contrasting IV-CEUS with MRI using histopathology as a reference are scarce. Therefore, further research is needed to clarify the diagnostic value and potential role of IV-CEUS in the EC staging algorithm.

This study aimed to evaluate the diagnostic performance of IV-CEUS compared to MRI in the preoperative assessment of myometrial invasion and CSI in EC, with the goal of assessing its potential as a practical alternative when MRI is unsuitable or unavailable.

Methods

Study design and subjects

This retrospective, single-center study was conducted at the Tianjin Central Hospital of Gynecology Obstetrics. A total of 71 patients who underwent surgery for histologically confirmed EC between January-2021 to August-2024 were enrolled in our study. All patients had undergone both IV-CEUS and MRI within 14 days before surgery. The study was conducted in accordance with the Declaration of He* lsinki and approved by the Ethics Committee of Tianjin Central Hospital of Gynecology Obstetrics (Approval No. 2021KY047). The requirement for informed consent was waived due to the retrospective nature of the study and the use of anonymized data.

Inclusion criteria: (1) Female patients aged 18-80 years; (2) Presenting with abnormal uterine bleeding; (3) transvaginal ultrasound showing endometrial thickening (> 10 mm in premenopausal women, > 4 mm in postmenopausal women); (4) Clinical suspicion of endometrial malignancy; (5) Completion of both IV-CEUS and MRI within 14 days prior to surgery; (6) Histologically confirmed endometrial carcinoma following surgical treatment; (7) Availability

of complete clinical, imaging, and pathological reports.

Exclusion criteria: (1) Cardiopulsion dysfunction or other major systemic disease; (2) Pregnancy or lactation; (3) History of preoperative radiotherapy, chemotherapy, or endocrine therapy; (4) Presence of intrauterine devices; (5) Other pelvic malignancies; (6) Poor image quality or incomplete clinical data; (7) Investigator decision for exclusion; (8) Incomplete postoperative data or loss to follow-up.

Sample size calculation

The sample size was estimated based on the primary aim of comparing the area under the receiver operating characteristic curve (AUC) between IV-CEUS and MRI for DMI detection. The calculation was performed using PASS 2021 (NCSS, LLC). Based on previous literature and pilot data, the expected AUC for MRI was set at 0.85, and for IV-CEUS at 0.80. With a significance level (α) of $\alpha = 0.05$, and power (1-β) of 80%, a minimum of 62 subjects was required. Accounting for potential dropouts or data exclusion rate of approximately 10%, a target sample size of 70 cases was determined. Ultimately, 71 patients were included in the final analysis, which met the calculated requirement.

Data collection

Clinical data were extracted from electronic medical records, including patient age, height, weight, body mass index (BMI), history of hypertension, diabetes and pregnancy, as well as imaging results, surgical details, and postoperative histopathological findings. All data were anonymized prior to analysis. Two independent investigators reviewed the data for completeness and accuracy, with discrepancies resolved by consensus.

IV-CEUS examination

Examinations were performed using high-end color Doppler ultrasound systems (Logiq E9, Voluson E8, and Voluson E10; GE Healthcare, Austria). Patients were positioned in the lithotomy or supine position based on the approach (transvaginal or abdominal). After initial grayscale and color Doppler scans to assess uterine size, lesion location, and vascularity, the contrast agent SonoVue® (Bracco Imaging S.p.A., Milan, Italy) was prepared according to manufacturer instructions and administered as a 2.4 mL intravenous bolus via the antecubital vein, followed by a 5 mL saline flush. Real-time CEUS imaging was performed in 3-5 minutes using a low mechanical index (MI < 0.1). Dynamic video clips and static images were acquired, and time-intensity curves (TICs) were generated to quantify perfusion parameters such as time to peak, peak intensity, wash-in and wash-out slopes, and enhancement homogeneity. Suspicious features for malignancy included heterogeneous enhancement, irregular wash-out, ill-defined borders, and myometrial fixation. All sonographers had over 10 years of experience in gynecologic imaging.

MRI protocol

MRI was performed on a 1.5 T Achieva scanner (Philips Healthcare, The Netherlands). The protocol included multiplanar T2-weighted imaging (T2WI), T1-weighted imaging (T1WI), diffusion-weighted imaging (DWI), and dynamic contrast-enhanced MRI (DCE-MRI). Patients were instructed to maintain a moderately full bladder to improve uterine visualization and reduce artifacts. Scanning parameters were as follows: sagittal T2WI (TR = 3000 ms, TE = 80 ms, slice thickness = 5 mm), axial and oblique T2WI (TR = 4200 ms, TE = 120 ms, slice thickness = 4 mm), axial T1WI (TR = 600 ms, TE = 10 ms, slice thickness = 4 mm), and DWI (b-values = 0 and 800 s/mm^2, slice thickness = 4 mm). For DCE-MRI, gadoterate meglumine (Gd-DOTA, Guidi-Xian®; Jiangsu Hengrui Pharmaceutical Co., Ltd.) was administered at 0.1 mmol/kg via a power injector at 2.0 mL/s, followed by a 20 mL saline flush. Five dynamic phases were acquired at 15-second intervals. Diagnostic parameters included tumor signal intensity and morphology on T2WI and DWI, enhancement kinetics on DCE-MRI, and junctional zone integrity.

Image interpretation standards and blinding

All IV-CEUS and MRI images were independently interpreted by two radiologists, each with over 10 years of experience in gynecologic imaging. The readers were blinded to the clinical data, pathological results, and, crucially, to the results of the other imaging modality (i.e., the MRI reader was blinded to IV-CEUS results and vice versa) to prevent interpretation bias.

For MRI, assessment of DMI and CSI followed the guidelines of the European Society of Urogenital Radiology (ESUR) [20]. DMI was defined as tumor extension ≥ 50% into the myometrial thickness, indicated on T2WI by disruption of the junctional zone and on DCE-MRI by interruption of the subendometrial enhancement band. CSI was diagnosed when tumor signal extended into the cervical stroma on T2WI, with corresponding enhancement on DCE-MRI and loss of the hypointense stromal ring.

For IV-CEUS, DMI was defined as the disruption of the continuous subendometrial enhancement ring and tumor extension ≥ 50% into the myometrium. Key features included an irregular, heterogeneous enhancement pattern of the lesion and an ill-defined tumor-myometrium interface. CSI was diagnosed by the loss of the normal cervical stromal enhancement ring and direct visualization of tumor extension into the cervical stroma. Rapid wash-in, high peak intensity, and early wash-out on TIC analysis were considered suggestive of malignancy.

In cases of disagreement between the two primary readers, a third senior radiologist was consulted, and a final decision was reached by consensus.

Hematoxylin and eosin (H & E)

Surgical specimens were fixed in 10% neutral-buffered formalin, processed routinely, and embedded in paraffin. Sections (4 μm thick) were stained with hematoxylin and eosin (H & E). Two board-certified pathologists with ≥ 10 years of experience in gynecologic oncology independently reviewed the slides, blinded to clinical and imaging data. Disagreements were resolved by consensus.

For the assessment of DMI, the entire uterus was sectioned along the longitudinal axis from the cervical os to the fundus. The maximum depth of tumor invasion was measured perpendicularly from the endometrial surface to the deepest point of invasion, and expressed as a percentage of the total myometrial thickness at that site. DMI was defined as invasion ≥ 50%. For CSI, the presence of tumor cells infiltrating the cervical stromal tissue was assessed. The intraclass correlation coefficient (ICC) for interobserver agreement in measuring the depth of myometrial invasion was 0.89 (excellent agreement), and the Kappa value for CSI assessment was 0.85 (almost perfect agreement).

Pathological staging was determined according to the International Federation of Gynecology and Obstetrics (FIGO) surgical staging system 2023 [21].

Statistical analysis

Statistical analyses were performed using SPSS 26.0 (IBM Corp., Armonk, NY, USA). Continuous variables were described as medians and ranges, while categorical variables were described using counts and percentages. Sensitivity, specificity, positive predictive value (PPV), and negative predictive value (NPV), and accuracy were assessed using McNemar's test. Agreement between imaging and histopathology was evaluated using Cohen's Kappa coefficient ($\kappa > 0.75$: excellent agreement; 0.40-0.75: moderate agreement; < 0.40: poor agreement). Receiver operating characteristic (ROC) curves were plotted, and areas under the curve (AUC) were compared using the DeLong test. A p-value < 0.05 was considered statistically significant.

Results

Patient characteristics

A total of 71 patients with histologically confirmed EC were included (**Table 1**). The median age was 56 years (range: 27-76), and the median BMI was 21.2 kg/m² (range: 18.0-30.1). Among them, 8 patients (11.3%) were nulliparous, 20 (28.2%) had hypertension, and 9 (12.7%) had diabetes mellitus. Histological differentiation included G1 in 37 patients (52.1%), G2 in 17 (23.9%), G3 in 6 (8.5%), and non-endometrioid histology in 11 (15.5%). According to the 2023 FIGO staging system, 35 patients (49.3%) were stage IA, 16 (22.5%) stage IB, 8 (11.3%) stage II, 2 (2.8%) stage IIIA, 3 (4.2%) stage IIIB, 5 (7.0%) stage IIIC, and 2 (2.8%) stage IVA. No patients were stage IVB.

Diagnostic performance for Deep Myometrial Invasion (DMI)

Histopathological examination confirmed DMI in 31 of the 71 patients (43.7%). The confusion

Table 1. Patient clinical characteristics and the final histological diagnoses (n = 71)

Characteristics	Value
Age (years)	56 (27-76)
BMI (kg/m²)	21.2 (18.0-30.1)
Nulliparous, n (%)	8 (11.3)
Hypertension, n (%)	20 (28.2)
Diabetes, n (%)	9 (12.7)
Histological grade, n (%)	
G1	37 (52.1)
G2	17 (23.9)
G3	6 (8.5)
Non-endometrioid	11 (15.5)
FIGO stage (2023), n (%)	
IA	35 (49.3)
IB	16 (22.5)
II	8 (11.3)
IIIA	2 (2.8)
IIIB	3 (4.2)
IIIC	5 (7.0)
IVA	2 (2.8)
IVB	0 (0.0)

Notes: Values are presented as median (min, max) or number (%). BMI, body mass index; FIGO, International Federation of Gynecology and Obstetrics.

matrices for IV-CEUS and MRI in diagnosing DMI are presented in **Table 2**. The diagnostic performance for DMI was calculated and is summarized in **Table 3**. For DMI, IV-CEUS showed a sensitivity of 74.2%, specificity of 92.5%, PPV of 88.5%, NPV of 82.2%, and accuracy of 84.5% (κ = 0.68). MRI demonstrated a sensitivity of 90.3%, specificity of 85.0%, PPV of 82.4%, NPV of 91.9%, and accuracy of 87.3% (κ = 0.75). There were no significant differences in sensitivity (P = 0.125), specificity (P = 0.289), or accuracy (P = 0.664) between the two modalities. ROC analysis yielded AUC values of 0.704 (95% CI: 0.584-0.824) for IV-CEUS and 0.718 (95% CI: 0.602-0.834) for MRI in diagnosing DMI (P < 0.001 for both), with no significant difference between them (P = 0.12) (**Figure 1A**).

Diagnostic performance for Cervical Stromal Invasion (CSI)

Histopathological examination confirmed CSI in 13 patients. The confusion matrices for IV-CEUS and MRI in diagnosing CSI are presented in **Table 4**. The diagnostic performance for CSI was calculated and is summarized in **Table 5**. IV-CEUS demonstrated a sensitivity of 69.2%, specificity of 93.1%, PPV of 69.2%, NPV of 93.1%, and accuracy of 88.7% (κ = 0.62). MRI showed a sensitivity of 76.9%, specificity of 87.9%, PPV of 58.8%, NPV of 94.4%, and accuracy of 85.9% (κ = 0.60). Differences in sensitivity (P = 0.687), specificity (P = 0.388), and accuracy (P = 0.607) were not statistically significant. ROC analysis yielded AUC values of 0.852 (95% CI: 0.743-0.961) for IV-CEUS and 0.838 (95% CI: 0.721-0.955) for MRI (P < 0.001 for both), with no significant difference (P = 0.078) (**Figure 1B**).

Subgroup analysis based on tumor grade

A subgroup analysis was performed to explore the association between IV-CEUS quantitative parameters and tumor differentiation grade (G1/G2/G3). The results indicated that high-grade tumors (G3) tended to exhibit a higher peak intensity and a shorter time to peak on TIC analysis compared to low-grade tumors (G1), although these differences did not reach statistical significance in all pairwise comparisons, likely due to the limited sample size in the G3 subgroup (n = 6). This preliminary finding suggests a potential correlation between aggressive tumor biology and distinct perfusion characteristics on IV-CEUS, warranting further investigation in larger cohorts.

Case presentation

Case 1: A 67-year-old woman with stage IA EC. Postoperative pathology revealed endometrioid adenocarcinoma with superficial myometrial invasion (< 50%) and no lymphovascular space invasion (**Figure 2A-C**). MRI showed an irregular intermediate-signal lesion in the endometrial cavity with heterogeneous enhancement on DCE-MRI, consistent with superficial invasion (**Figure 2D-F**). IV-CEUS revealed heterogeneous enhancement and a disrupted endometrial-myometrial junction (**Figure 2G-I**).

Case 2: A 54-year-old woman with stage II EC. Postoperative pathology confirmed grade III endometrioid adenocarcinoma with CSI (**Figure 3A-C**). MRI demonstrated an intermediate T2WI signal, DWI hyperintensity, and heterogeneous enhancement on DCE-MRI, suggesting CSI (**Figure 3D-F**). IV-CEUS showed rapid wash-in, high peak intensity, and blurred endometri-

Table 2. Confusion matrices for DMI detection

Modality	Histopathology: DMI+	Histopathology: DMI-
IV-CEUS+	23 (True Positive)	3 (False Positive)
IV-CEUS-	8 (False Negative)	37 (True Negative)
MRI+	28 (True Positive)	6 (False Positive)
MRI-	3 (False Negative)	34 (True Negative)

al-myometrial and endocervical interfaces (**Figure 3G-I**).

Discussion

This study demonstrates that IV-CEUS possesses comparable diagnostic performance to MRI in preoperative staging of DMI and CSI in EC patients. This finding holds significant clinical relevance, as it substantiates the role of IV-CEUS as a viable and accessible alternative for patients who cannot undergo MRI.

The high specificity (92.5% for DMI, 93.1% for CSI) and positive predictive value of IV-CEUS are particularly noteworthy. These metrics are critical in a preoperative setting, as a positive finding on IV-CEUS can strongly indicate the need for more radical surgery (e.g., hysterectomy with lymphadenectomy for DMI, or radical hysterectomy for CSI), thereby directly influencing surgical planning and potentially improving patient outcomes [22, 23]. While demonstrating higher sensitivity, the slightly lower specificity of MRI could lead to false positives, potentially resulting in overtreatment. The performance profile of IV-CEUS suggests that it is an excellent "rule-in" modality. The high specificity of IV-CEUS may be attributed to its ability to vividly depict microvascular architecture and real-time perfusion. The microbubble contrast agents used in IV-CEUS are purely intravascular, making them highly sensitive to neovascularization and abnormal vascular patterns associated with malignant invasion [24]. This direct visualization of functional blood flow might allow IV-CEUS to more accurately distinguish true stromal invasion from benign conditions like inflammation or edema, which can sometimes mimic invasion on MRI due to T2-weighted signal changes or non-specific enhancement.

Furthermore, our exploratory subgroup analysis suggested a trend towards association between specific IV-CEUS perfusion parameters (e.g., higher peak intensity) and higher tumor grade. This aligns with the understanding that more aggressive tumors often exhibit increased angiogenesis and vascular density [25]. While preliminary and limited by sample size, this finding highlights the potential of IV-CEUS quantitative parameters to serve as non-invasive biomarkers for tumor aggressiveness, extending its value beyond morphological assessment.

The clinical applicability of IV-CEUS is especially pronounced in specific patient populations. For obese patients, ultrasound is often less affected by body habitus compared to MRI, which can suffer from signal attenuation [26]. In patients with renal insufficiency, IV-CEUS uses microbubble contrast agents (SonoVue®) that are not nephrotoxic and are safe for use, unlike gadolinium-based MRI contrast agents which carry a risk of nephrogenic systemic fibrosis [17]. Furthermore, the real-time nature of IV-CEUS allows for dynamic assessment of tumor perfusion and tumor margins during the examination, which can be advantageous for targeted biopsies and assessing tumor vascularity. From a economic perspective, IV-CEUS is significantly more cost-effective than MRI, requires less space, and has shorter examination times, making it particularly suitable for resource-limited settings or high-volume centers [17].

The slightly lower sensitivity of IV-CEUS for detecting CSI (69.2% vs. 76.9% for MRI) warrants discussion. This is likely attributable to the inherent anatomical and technical limitations of ultrasound in evaluating the cervix, particularly its lower soft-tissue contrast resolution compared to MRI [27]. The cervix's complex anatomy and the potential for shadowing from overlying bowel gas can sometimes obscure clear visualization of stromal invasion. Future technical improvements, such as the development of high-frequency transvaginal CEUS probes or the use of 3D CEUS acquisition, could potentially enhance the visualization of the cervico-isthmic region. Moreover, a combined approach using conventional transvaginal ultrasound for anatomical overview and IV-CEUS for microvascular assessment might synergistically improve diagnostic accuracy for CSI [28].

Table 3. Diagnostic performance of IV-CEUS and MRI for deep myometrial invasion (DMI)

Modality	Sensitivity (%)	Specificity (%)	PPV (%)	NPV (%)	Accuracy (%)	Kappa (κ)
IV-CEUS	74.2	92.5	88.5	82.2	84.5	0.68
MRI	90.3	85.0	82.4	91.9	87.3	0.75

Notes: Values are presented as % (95% CI), IV-CEUS, intravenous contrast-enhanced ultrasound; DMI, deep myometrial invasion (≥ 50%); CI, confidence interval; MRI, magnetic resonance imaging; PPV, positive predictive value; NPV, negative predictive value.

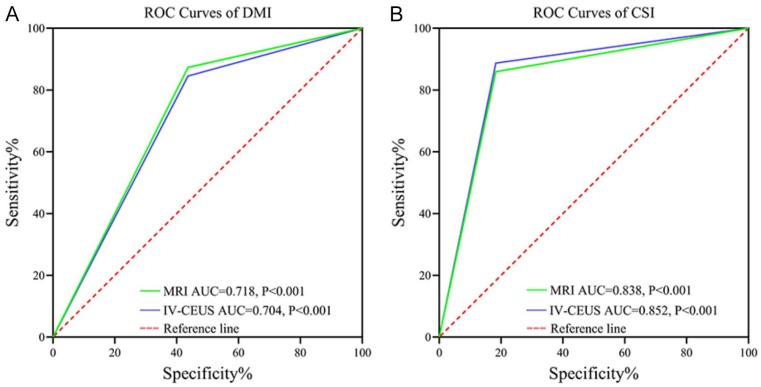

Figure 1. ROC curve analysis for MRI and IV-CEUS in diagnosing DMI (A) and CSI (B) in EC patients. AUC, area under the curve; ROC, receiver operating characteristic; MRI, magnetic resonance imaging; IV-CEUS, intravenous contrast-enhanced ultrasound; DMI, deep myometrial invasion; CSI, cervical stromal invasion.

Table 4. Confusion matrices for CSI detection

Modality	Histopathology: CSI+	Histopathology: CSI-
IV-CEUS+	9 (True Positive)	4 (False Positive)
IV-CEUS-	4 (False Negative)	54 (True Negative)
MRI+	10 (True Positive)	7 (False Positive)
MRI-	3 (False Negative)	51 (True Negative)

Our study has several limitations that should be acknowledged. First, its retrospective and single-center design may introduce selection bias and limit the generalizability of the findings. Second, the sample size, though sufficient for the primary aim, resulted in a relatively small number of CSI-positive cases (n = 13). This small subgroup size may affect the robustness of the sensitivity for CSI and reduces the statistical power for this specific analysis. Third, as a retrospective study, systematic data on molecular biomarkers of angiogenesis (e.g., VEGF, CD31) from tumor tissues are lacking, which prevented a direct correlation analysis between IV-CEUS parameters and underlying molecular mechanisms. Future prospective studies integrating histopathological and molecular data are needed to fully elucidate the biological basis of IV-CEUS findings. Fourth, while IV-CEUS shows great promise, it remains operator-dependent. Although all operators in this study were highly experienced, the results might vary in less specialized settings. Standardized training protocols would be essential for wider implementation.

Future prospective, multicenter studies with larger sample sizes are needed to validate our findings and to establish standardized IV-CEUS protocols for EC staging. Integrating artificial intelligence (AI) for the analysis of CEUS time-intensity curves and enhancement patterns could further reduce operator dependency and improve diagnostic reproducibility [29]. Furthermore, future research should explore the value of quantitative IV-CEUS parameters as potential biomarkers for predicting tumor grade, lymph node metastasis, and therapeutic response.

Conclusion

IV-CEUS possesses comparable diagnostic performance to MRI in preoperative assessment of DMI and CSI in EC patients. Given its high specificity, real-time capability, safety profile, and cost-effectiveness, IV-CEUS represents a valuable complementary imaging tool. It is a practical alternative for preoperative staging in patients with contraindications to MRI, such as those with renal impairment, severe claustrophobia, or metallic implants, as well as in resource-constrained environments. We recom-

Table 5. Diagnostic performance of IV-CEUS and MRI for cervical stromal invasion (CSI)

Modality	Sensitivity (%)	Specificity (%)	PPV (%)	NPV (%)	Accuracy (%)	Kappa (κ)
IV-CEUS	69.2	93.1	69.2	93.1	88.7	0.62
MRI	76.9	87.9	58.8	94.4	85.9	0.60

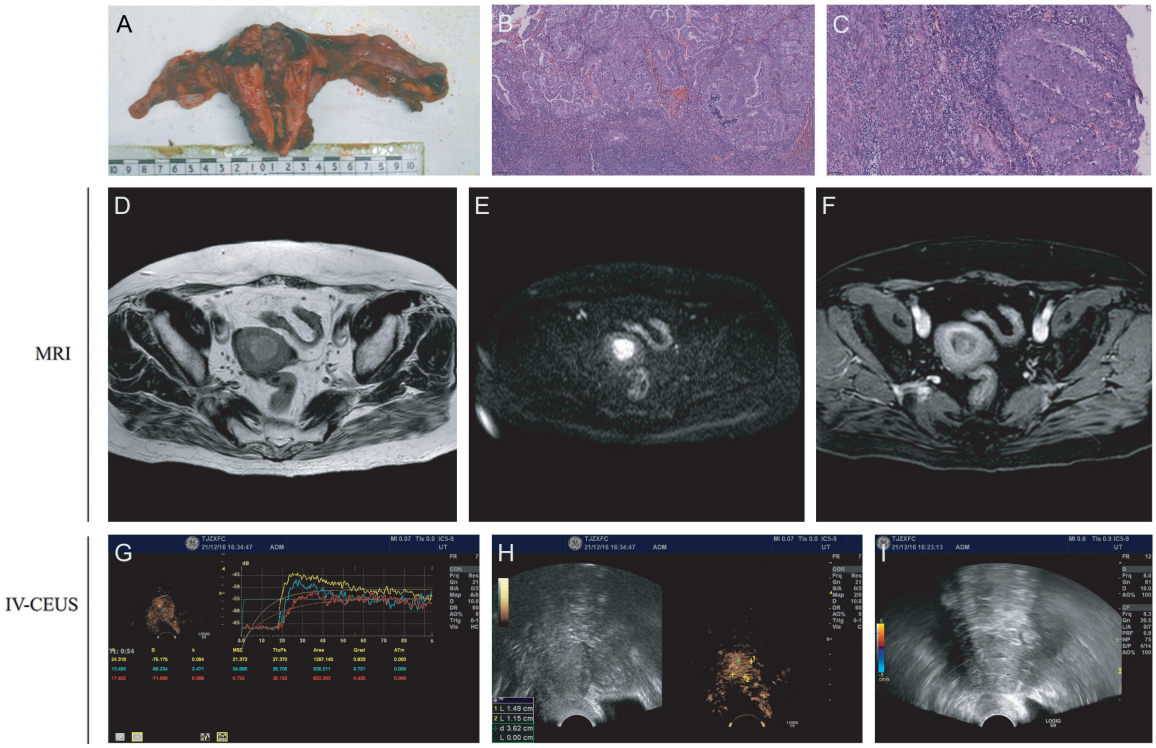

Figure 2. Representative MR, IV-CEUS, and histopathological images of stage IA EC. A. Gross specimen showing a tumor occupying the endometrial cavity. B. HE staining revealing moderately differentiated endometrioid adenocarcinoma (Original magnification: ×100). C. HE staining showing DMI (< 50%) and dense lymphocytic infiltration (Original magnification: ×200). D. Axial T2WI showing an irregular intermediate signal lesion. E. DWI revealing marked hyperintensity, indicating restricted diffusion. F. DCE-MRI showing mild heterogeneous enhancement, lower than surrounding myometrium. G. TIC from IV-CEUS showing rapid wash-in with a plateau phase, suggesting hypervascularity. H. Grayscale (left) and CEUS (right) images displaying a hypoechoic lesion with irregular margins and heterogeneous perfusion. I. Color Doppler showing diffuse endometrial thickening and a disrupted endometrial–myometrial junction. MRI, magnetic resonance imaging; T2WI, T2-weighted image; DWI, diffusion-weighted imaging; DCE-MRI, dynamic contrast-enhanced MRI; CEUS, contrast-enhanced ultrasound; IV-CEUS, intravenous contrast-enhanced ultrasound; TIC, time-intensity curve; DMI, deep myometrial invasion; EC, endometrial carcinoma; H & E, hematoxylin and eosin.

mend its further integration into clinical practice. Future prospective multicenter studies should focus on standardizing examination protocols, exploring the role of AI, validating its impact on treatment planning and patient outcomes, and investigating the correlation between quantitative perfusion parameters and molecular markers of tumor aggressiveness.

Acknowledgements

The work was funded by Tianjin Key Medical Discipline (Specialty) Construction Project (NO. TJYXZDXK-009A).

Disclosure of conflict of interest

None.

Address correspondence to: Zhaoxiang Ye, Department of Radiology, Tianjin Medical University Cancer Institute and Hospital, National Clinical Research Center for Cancer; Tianjin's Clinical Research Center for Cancer; State Key Laboratory of Druggability Evaluation and Systematic Translational Medicine; Key Laboratory of Cancer Prevention and Therapy, Huanhuxi Road, Hexi District, Tianjin 300060, China. Tel: +86-022-23340123; E-mail: yezhaoxiang@163.com

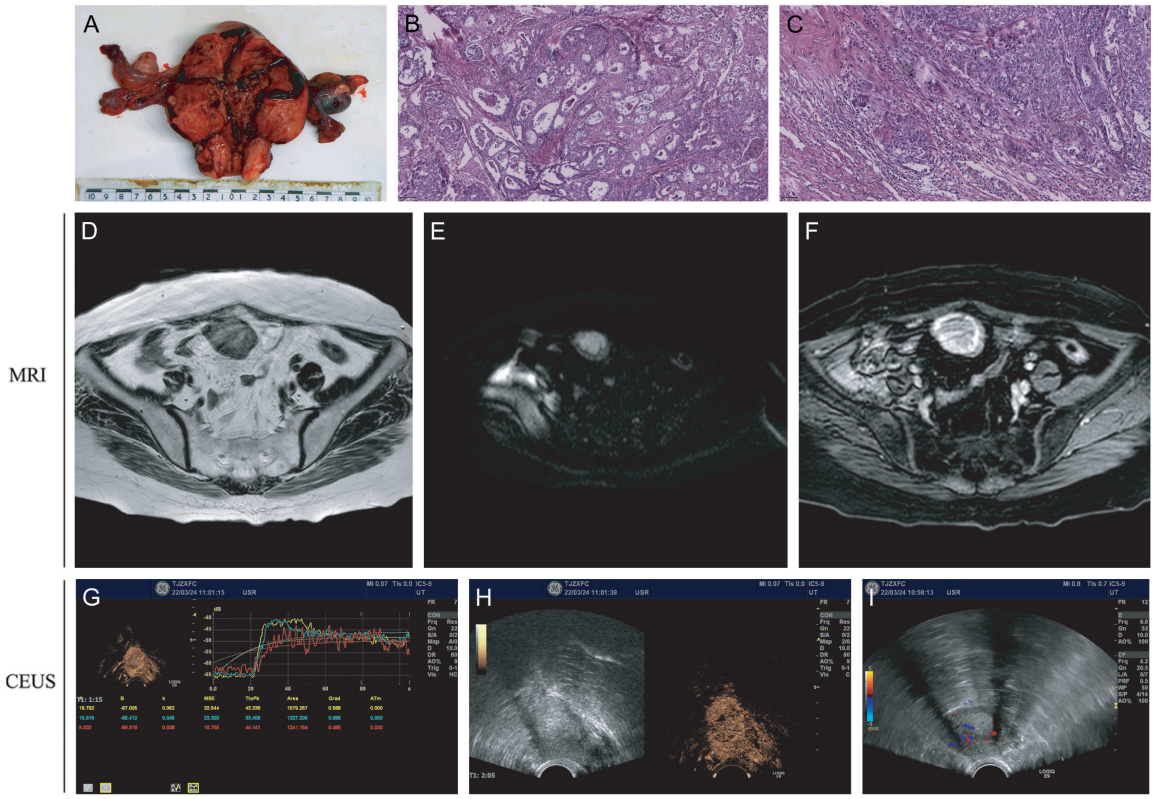

Figure 3. Representative MR, IV-CEUS, and histopathological images of stage II EC. A. Gross surgical specimen showing a tumor involving the endometrial cavity and extending toward the cervix. B. H & E staining revealing grade III endometrioid adenocarcinoma with cribriform glandular architecture and nuclear atypia (Original magnification: ×100). C. H & E image confirming stromal invasion of the cervix (Original magnification: ×200). D. Axial T2WI showing an irregular intermediate-signal lesion disrupting the junctional zone. E. DWI demonstrating hyperintensity in the lesion, suggesting restricted diffusion. F. DCE-MRI revealing heterogeneous enhancement and indistinct borders between the lesion and the surrounding myometrium and cervix. G. TIC derived from IV-CEUS displaying a rapid wash-in and high peak intensity, indicating increased tumor perfusion. H. Grayscale (left) and IV-CEUS (right) images showeding a hyperechoic intrauterine lesion with irregular margins and heterogeneous enhancement. I. Color Doppler ultrasound showing prominent vascularity and blurred delineation of the endometrial-myometrial and endocervical stromal interface. MRI, magnetic resonance imaging; T2WI, T2-weighted image; DWI, diffusion-weighted imaging; DCE-MRI, dynamic contrast-enhanced MRI; CEUS, contrast-enhanced ultrasound; IV-CEUS, intravenous contrast-enhanced ultrasound; TIC, time-intensity curve; EC, endometrial carcinoma; CSI, cervical stromal invasion; H & E, hematoxylin and eosin.

References

[1] Gu B, Shang X, Yan M, Li X, Wang W, Wang Q and Zhang C. Variations in incidence and mortality rates of endometrial cancer at the global, regional, and national levels, 1990-2019. Gynecol Oncol 2021; 161: 573-580.

[2] Pan X, Li J, Liu P, Li J, Zhao M, Wu Y, Ji S, Ren T, Jiang Q and Zhang S. Global trends in endometrial cancer and metabolic syndrome research: a bibliometric and visualization analysis. Comput Biol and Med 2025; 192: 110362.

[3] Turashvili G and Hanley K. Practical updates and diagnostic challenges in endometrial carcinoma. Arch Pathol Lab Med 2024; 148: 78-98.

[4] Török P, Krasznai Z, Molnár S, Lampé R and Jakab A. Preoperative assessment of endometrial cancer. Transl Cancer Res 2020; 9: 7746.

[5] McEachron J, Marshall L, Zhou N, Tran V, Kanis MJ, Gorelick C and Lee YC. Evaluation of survival, recurrence patterns and adjuvant therapy in surgically staged high-grade endometrial cancer with retroperitoneal metastases. Cancers (Basel) 2021; 13: 2052.

[6] Huvila J, Pors J, Thompson EF and Gilks CB. Endometrial carcinoma: molecular subtypes, precursors and the role of pathology in early diagnosis. J Pathol 2021; 253: 355-365.

[7] Choi S, Joo JW, Do SI and Kim HS. Endometrium-limited metastasis of extragenital malig-

nancies: a challenge in the diagnosis of endometrial curettage specimens. Diagnostics (Basel) 2020; 10: 150.
[8] Zandrino F, La Paglia E and Musante F. Magnetic resonance imaging in local staging of endometrial carcinoma: diagnostic performance, pitfalls, and literature review. Tumori 2010; 96: 601-608.
[9] Maheshwari E, Nougaret S, Stein EB, Rauch GM, Hwang KP, Stafford RJ, Klopp AH, Soliman PT, Maturen KE and Rockall AG, Lee SI, Sadowski EA and Venkatesan AM. Update on MRI in evaluation and treatment of endometrial cancer. Radiographics 2022; 42: 2112-2130.
[10] Antonova IB, Aksenova SP, Nudnov NV and Kriger AV. Possibilities and limitations of magnetic resonance imaging in the diagnostics of endocervical adenocarcinomas. Digit Diagn 2024; 5: 149-166.
[11] Xu X, Li N, Chen Y, Ouyang H, Zhao X and Zhou J. Diagnostic efficacy of MRI for pre-operative assessment of ovarian malignancy in endometrial carcinoma: a decision tree analysis. Magn Reson Imaging 2019; 57: 285-292.
[12] Dietrich CF, Correas J-M, Cui X-W, Dong Y, Havre RF, Jenssen C, Jung EM, Krix M, Lim A and Lassau N. EFSUMB technical review-update 2023: dynamic contrast-enhanced ultrasound (DCE-CEUS) for the quantification of tumor perfusion. Ultraschall Med 2024; 45: 36-46.
[13] Piscaglia F, Nolsoe C, Dietrich CF, Cosgrove DO, Gilja OH, Bachmann Nielsen M, Albrecht T, Barozzi L, Bertolotto M, Catalano O, Claudon M, Clevert DA, Correas JM, D'Onofrio M, Drudi FM, Eyding J, Giovannini M, Hocke M, Ignee A, Jung EM, Klauser AS, Lassau N, Leen E, Mathis G, Saftoiu A, Seidel G, Sidhu PS, ter Haar G, Timmerman D and Weskott HP. The EFSUMB guidelines and recommendations on the clinical practice of contrast enhanced ultrasound (CEUS): update 2011 on non-hepatic applications. Ultraschall Med 2012; 33: 33-59.
[14] Testa AC, Timmerman D, Van Belle V, Fruscella E, Van Holsbeke C, Savelli L, Ferrazzi E, Leone FP, Marret H, Tranquart F, Exacoustos C, Nazzaro G, Bokor D, Magri F, Van Huffel S, Ferrandina G and Valentin L. Intravenous contrast ultrasound examination using contrast-tuned imaging (CnTI) and the contrast medium SonoVue for discrimination between benign and malignant adnexal masses with solid components. Ultrasound Obstet Gynecol 2009; 34: 699-710.
[15] Zhuang L, Ming X, Liu J, Jia C, Jin Y, Wang J, Shi Q, Wu R, Jin L and Du L. Comparison of lymphatic contrast-enhanced ultrasound and intravenous contrast-enhanced ultrasound in the preoperative diagnosis of axillary sentinel lymph node metastasis in patients with breast cancer. Br J Radiol 2022; 95: 20210897.
[16] Sidhu PS, Cantisani V, Dietrich CF, Gilja OH, Saftoiu A, Bartels E, Bertolotto M, Calliada F, Clevert DA, Cosgrove D, Deganello A, D'Onofrio M, Drudi FM, Freeman S, Harvey C, Jenssen C, Jung EM, Klauser AS, Lassau N, Meloni MF, Leen E, Nicolau C, Nolsoe C, Piscaglia F, Prada F, Prosch H, Radzina M, Savelli L, Weskott HP and Wijkstra H. The EFSUMB guidelines and recommendations for the clinical practice of contrast-enhanced ultrasound (CEUS) in non-hepatic applications: update 2017 (Long Version). Ultraschall Med 2018; 39: e2-e44.
[17] Najjar R. Clinical applications, safety profiles, and future developments of contrast agents in modern radiology: a comprehensive review. Iradiology 2024; 2: 430-468.
[18] Fang C, Anupindi SA, Back SJ, Franke D, Green TG, Harkanyi Z, Jüngert J, Kwon JK, Paltiel HJ, Squires JH, Zefov VN and McCarville MB. Contrast-enhanced ultrasound of benign and malignant liver lesions in children. Pediatr Radiol 2021; 51: 2181-2197.
[19] Huang C, Luo J, Shan Z, Zhen T, Li J, Ma Q, Wei L, Liang J, Xie X and Zheng Y. The value of the improved percutaneous and intravenous contrast-enhanced ultrasound diagnostic classification in sentinel lymph nodes of breast cancer. Quant Imaging Med Surg 2024; 14: 2391-2404.
[20] Kubik-Huch RA, Weston M, Nougaret S, Leonhardt H, Thomassin-Naggara I, Horta M, Cunha TM, Maciel C, Rockall A and Forstner R. European Society of Urogenital Radiology (ESUR) guidelines: MR imaging of leiomyomas. Eur Radiol 2018; 28: 3125-3137.
[21] Berek JS, Matias-Guiu X, Creutzberg C, Fotopoulou C, Gaffney D, Kehoe S, Lindemann K, Mutch D and Concin N; Endometrial Cancer Staging Subcommittee FWsCC; FIGO Women's Cancer Committee. FIGO staging of endometrial cancer: 2023. Int J Gynecol Obstet 2023; 162: 383-394.
[22] Njoku K, Chiasserini D, Whetton AD and Crosbie EJ. Proteomic biomarkers for the detection of endometrial cancer. Cancers (Basel) 2019; 11: 1572.
[23] Al Khatib S, Bhatnagar A, Elshaikh N, Ghanem AI, Burmeister C, Allo G, Alkamachi B, Paridon A and Elshaikh MA. The prognostic significance of the depth of cervical stromal invasion in women with FIGO stage II uterine Endometrioid carcinoma. Am J Clin Oncol 2023; 46: 445-449.
[24] Jianxiong W, Yu W, Juyi W and Guangxia W. Intravenous combined with intrabiliary contrast-enhanced ultrasound in the evaluation of resectability of hilar cholangiocarcinomas. J Clin Ultrasound 2022; 50: 931-939.

[25] Maiques O, Sallan MC, Laddach R, Pandya P, Varela A, Crosas-Molist E, Barcelo J, Courbot O, Liu Y, Graziani V, Arafat Y, Sewell J, Rodriguez-Hernandez I, Fanshawe B, Jung-Garcia Y, Imbert PR, Grasset EM, Albrengues J, Santacana M, Macia A, Tarragona J, Matias-Guiu X, Marti RM, Tsoka S, Gaggioli C, Orgaz JL, Fruhwirth GO, Wallberg F, Betteridge K, Reyes-Aldasoro CC, Haider S, Braun A, Karagiannis SN, Elosegui-Artola A and Sanz-Moreno V. Matrix mechano-sensing at the invasive front induces a cytoskeletal and transcriptional memory supporting metastasis. Nat Commun 2025; 16: 1394.

[26] Zhang Q, Yao Y, Yu Z, Zhou T, Zhang Q, Li H, Zhang J, Wei S, Zhang T and Wang H. Bioinformatics analysis and experimental verification define different angiogenesis subtypes in endometrial carcinoma and identify a prognostic signature. ACS Omega 2024; 9: 26519-26539.

[27] Miele V, Piccolo CL, Galluzzo M, Ianniello S, Sessa B and Trinci M. Contrast-enhanced ultrasound (CEUS) in blunt abdominal trauma. Br J Radiol 2016; 89: 20150823.

[28] Huang JW, Zeng H, Zhang Q, Liu XY and Feng C. Advances in the clinical diagnosis of lung cancer using contrast-enhanced ultrasound. Front Med (Lausanne) 2025; 12: 1543033.

[29] Zhang J and Dawkins A. Artificial intelligence in ultrasound imaging: where are we now? Ultrasound Q 2024; 40: 93-97.